Photochemical & Photobiological Sciences

Accepted Manuscript

This is an *Accepted Manuscript*, which has been through the Royal Society of Chemistry peer review process and has been accepted for publication.

Accepted Manuscripts are published online shortly after acceptance, before technical editing, formatting and proof reading. Using this free service, authors can make their results available to the community, in citable form, before we publish the edited article. We will replace this *Accepted Manuscript* with the edited and formatted *Advance Article* as soon as it is available.

You can find more information about *Accepted Manuscripts* in the Information for Authors.

Please note that technical editing may introduce minor changes to the text and/or graphics, which may alter content. The journal's standard Terms & Conditions and the Ethical guidelines still apply. In no event shall the Royal Society of Chemistry be held responsible for any errors or omissions in this *Accepted Manuscript* or any consequences arising from the use of any information it contains.

ROYAL SOCIETY OF CHEMISTRY

www.rsc.org/pps

Photochemical &
Photobiological Sciences

RSCPublishing

PAPER

Enhanced photostability of an anthracene-based dye due to supramolecular encapsulation: A new type of photostable fluorophore for single-molecule study

Masaaki Mitsui,* Koji Higashi, Ryoya Takahashi, Yohei Hirumi, Kenji Kobayashi

Cite this: DOI: 10.1039/xoxx000000x

Received ooth February 2014,
Accepted ooth xxx 2014

DOI: 10.1039/xoxx000000x

www.rsc.org/pps

For single-molecule fluorescence studies, highly photostable fluorophores are absolutely imperative, because photo-induced degradation (i.e., photobleaching) limits the observation time of individual molecules. Herein, the photophysics and photostability of a highly fluorescent 9,10-bis(phenylethynyl)anthracene derivative (G) and its self-assembled boronic ester encapsulation complex (G@Cap) embedded in a glassy polymer matrix are investigated by single-molecule fluorescence spectroscopy (SMFS). The heterogeneity of the fluorescence emission wavelength and triplet blinking kinetics of the guest G are significantly decreased by supramolecular encapsulation due to conformational restriction and reduced heterogeneity in the local environment. A nearly 10-fold increase in the photostability of G due to encapsulation is quantitatively confirmed by evaluating the photobleaching yields of G and G@Cap. In addition, it is found that the G@Cap is >30-fold more photostable than rhodamine 6G, a widely used fluorescent dye in single-molecule studies. These results demonstrate the G@Cap can serve as a very bright, long-lasting fluorescent probe for single-molecule studies.

Introduction

Photostable organic fluorophores that enable prolonged single-molecule detection are becoming increasingly indispensable in broad areas of advanced research that use fluorescence-based single-molecule techniques such as single-molecule fluorescence spectroscopy (SMFS),[1,2] single-molecule orientation imaging[1-3] and single-molecule super-resolution microscopy.[4] However, organic fluorophores undergo photon-induced chemical damage and permanently lose their ability to fluoresce; this phenomenon is called photobleaching. Recently, several efforts have been devoted to suppress photobleaching and enhance fluorophore photostability in single-molecule fluorescence measurements.[5-9] The use of triplet-state quenchers,[5-7] microfluidic device,[8] and micrometer-sized polydimethylsiloxane wells[9] successfully enhance the photostability of fluorophores. Supramolecular encapsulation has also been widely recognized as a photostabilization strategy. For example, increment in the photostability of fluorescent guest has been achieved using cyclodextrins,[10-12] cucurbit[n]urils,[13,14] rotaxanes,[10,11,15] and self-assembled molecular capsules.[16-20] However, this strategy has been preponderantly utilized for organic fluorophores that are not bright enough for detection at the single-molecule level.

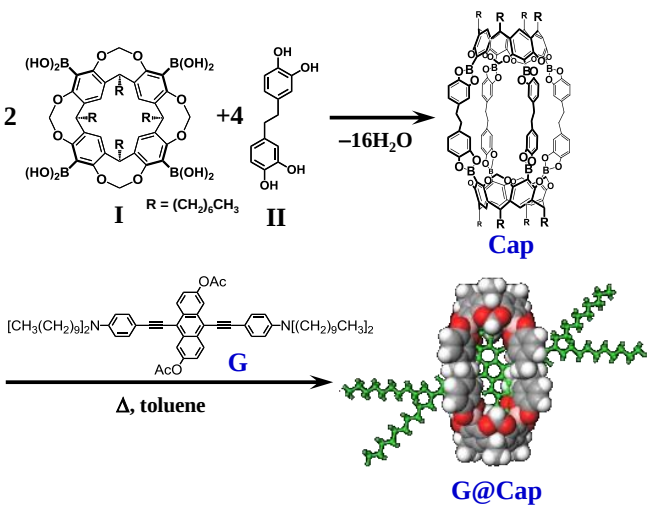

Scheme 1. Encapsulation of a BPEA derivative (G) in boronic ester cavitand capsule (Cap) self-assembled by **I** and **II**. The alkyl chains of Cap are replaced by methyl groups.

Kobayashi and co-workers[19] recently reported encapsulation of anthracene-based dyes in the self-assembled boronic ester cavitand capsule (Cap), which is generated as a result of the dynamic boronic ester formation between the cavitand tetraboronic acid **I** and the bis(catechol)-linker **II** (Scheme 1). They revealed that the Cap serves as a protective molecular container for the encapsulated guests. More recently, they also succeeded in producing supramolecular complexes encapsulating highly fluorescent 9,10-bis(phenylethynyl)anthracene (BPEA) derivatives,[20] one of which (hereafter G) is depicted in Scheme 1. BPEA and its derivatives are known to be highly fluorescent,[21,22] and it has been recently shown that BPEA meets the essential requirements for SMFS studies, such as high fluorescence quantum yields (Φ_f) and reasonably low photobleaching yields (Φ_b).[23] G also possesses a large molar absorption coefficient (ε_{max} = 45,800 $M^{-1}cm^{-1}$ at 494 nm in toluene) and high fluorescence quantum yield (Φ_f = 0.97 in toluene), which are superior to those of BPEA (ε_{max} ~33,000 $M^{-1}cm^{-1}$ at 451 nm and Φ_f ~ 0.93).[21-23] More importantly, upon encapsulation of G, the molar absorption coefficient is enhanced (ε_{max} = 60,300 $M^{-1}cm^{-1}$ at 541 nm in toluene), while the fluorescence quantum yield remains almost unchanged (Φ_f = 0.94 in toluene).[20] In addition to the excellent one-photon absorption/fluorescence property, the encapsulation complex G@Cap also has a good two-photon absorption property.[20] Thus, G@Cap is expected to serve as a novel class of fluorescent probes with high brightness and high photostability. In this report, we quantitatively evaluate the effects of supramolecular encapsulation by the Cap on the photophysics and photostability of the guest G at the single-molecule level.

Experimental

Sample preparation

The nonpolar cyclo-olefin polymer Zeonex (T_g = 123 °C, Zeon Chemicals); methylcyclohexane (MCH), which has a dielectric constant (2.02), comparable to that of Zeonex (2.3); and toluene (spectroscopic grade, Wako) were used as received. Ensemble absorption spectra of G and G@Cap in MCH were recorded on a spectrometer (Lambda 650, Perkin-Elmer), and fluorescence spectra were obtained with a RF-5300PC fluorometer (Shimadzu) and a liquid-nitrogen-cooled charge-coupled device (CCD) camera that was coupled to a polychromator. Rhodamine 6G (R6G) was purchased from Wako and used as received. G and Cap were synthesized as described elsewhere.[20] The association constant (K_a) of G@Cap was extremely large (2.12×10^7 M^{-1} in C_6D_6 at 313 K),[20] so a low concentration of Cap (10–100 μM) is sufficient to ensure almost 100% encapsulation of G (~10^{-10} M) in toluene. A sample for single-molecule experiments was typically prepared by spin-coating one drop of a toluene solution containing G or G@Cap (~10^{-10} M) and Zeonex (10 mg/mL) onto thoroughly cleaned cover glasses. The resulting thickness of the doped polymer films amounts to 200 nm, as measured by atomic force microscopy (SPM-9700, Shimadzu).

Single-molecule fluorescence spectroscopy (SMFS)

Our home-made SMFS apparatus is described elsewhere.[23] Briefly, a continuous wave argon ion laser (177G, Spectra Physics) was used to excite the dye molecules at 488 nm. After elimination of residual plasma lines by laser-line filters and variable attenuation, the expanded and linearly polarized laser beam was guided into an oil immersion objective (100×, NA 1.4, Olympus), which focused the beam to a diffraction-limited spot in the sample plane. Average excitation intensities were 100–500 W/cm^2, which correspond to the excitation rate (k_{ex}) of 10^4–10^5 s^{-1} for G and G@Cap. The sample substrates were mounted on an O-ring and acted as the top face of a small vacuum chamber. During SMFS measurements, the sample side was placed in vacuum (<0.1 Pa) to remove oxygen in the polymer film. The collected fluorescence photons were separated from the excitation beam using a dichroic mirror (LPD01-488RU-25, Semrock), notch filter (NF03-488E-25, Semrock), and long-pass filter (LP02-488RE-25, Semrock). Note that this filter set can transmit photons of all the wavelengths that constitute fluorescence spectra of G and G@Cap. Subsequently, they were split by a 50:50 unpolarized beam splitter. Half of the detected fluorescence signal was recorded with a liquid-nitrogen-cooled charge-coupled device (CCD) camera that was coupled to a polychromator. The other half was focused onto a 75 mm pinhole for rejection of out-of-focus background and finally detected by an avalanche photodiode (APD, SPCM-AQR-14, Perkin-Elmer). The data were acquired using a time-correlated single-photon counting card (TimeHarp 200, PicoQuant) in a time-tagged time-resolved (T3R) mode, which stores all the relevant information for each detected single photon for further data analysis.

Data for the individual autocorrelation curves were analyzed using the software SymPhoTime (PicoQuant). The total detection efficiency at the APD in our setup was estimated to be ~4% by considering the transmission of all of the optical parts used in the detection path and the quantum efficiency of the APD detector. The spectral trajectories (3 s/spectrum) were recorded to verify that the observed signals originated from the single molecule of interest. To determine the wavelength of the fluorescence maximum (λ_{max}), each spectrum was fitted with the appropriate number of Gaussian functions. All measurements were conducted at room temperature.

Results and discussion

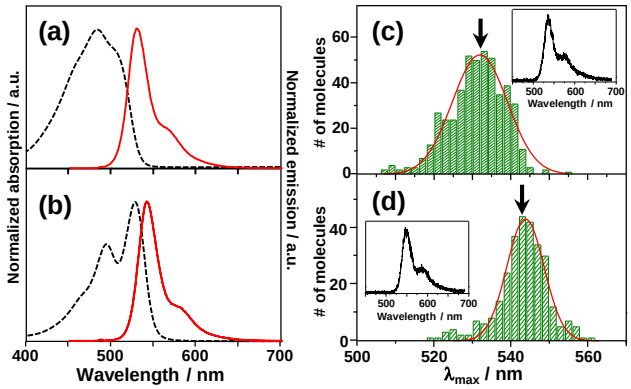

Fig.1 Normalized absorption and emission (excitation wavelength of 400 nm) spectra of (a) G and (b) G@Cap in MCH. Frequency histograms for wavelength of maximum emission (λ_{max}) of (c) G (475 molecules) and (d) G@Cap (459 molecules) in a Zeonex film. In (c) and (d), insets display typical single-molecule fluorescence spectra, and arrows indicate the corresponding λ_{max} in MCH (i.e., 532 nm for G and 543 nm for G@Cap).

Fig. 1a shows the UV–vis absorption and fluorescence spectra of G in MCH, while Fig. 1b shows those of G@Cap in MCH. The shape of G's fluorescence spectrum differs considerably from that of its absorption spectrum (*i.e.*, they are far from being mirror images). As with BPEA, the existence of a variety of conformations of G, in which the two arylethynyl groups can rotate almost freely in solution, contributes to its absorption spectrum, whereas a specific conformation (*e.g.*, the planar conformation) is mostly responsible for the fluorescence spectrum.[21] In contrast, the absorption spectrum of G@Cap clearly shows the partially resolved vibrational structure, indicating that the rotation of arylethynyl groups is highly restricted in the encapsulation complex.[20] While the overall spectral shape remains unchanged, the wavelength of the fluorescence maximum (λ_{max}) is red-shifted by 11 nm when G is included in the capsule. This red shift is attributed to the interaction of the arylethynyl groups of the guest with the catechol linkers of Cap, which stabilizes $S_1(\pi,\pi^*)$ state in G.[20] Hence, the λ_{max} value can serve as a useful parameter to distinguish encapsulated and non-encapsulated G in a polymer film.

Figs. 1c and 1d show the distribution of λ_{max} for single G and G@Cap molecules in Zeonex films, respectively, together with an example of a single-molecule fluorescence spectrum. The widths and mean values of the λ_{max} distributions differ significantly. Notably, each mean value of λ_{max} obtained by Gaussian fits (i.e., 532 nm for G and 545 nm for G@Cap) shows excellent agreement with the corresponding λ_{max} value in MCH. In addition, the FWHM of the λ_{max} distribution for G@Cap in Zeonex film (9.9 nm) is narrower than that for free G in Zeonex film (12.5 nm), which is attributed to the reduction in structural heterogeneity (*e.g.*, conformational restriction) of the guest on encapsulation and/or reduction in the environmental heterogeneity of the capsule's interior compared with that of Zeonex. These differences strongly indicate that most of the G@Cap molecules maintain the encapsulated form in the Zeonex matrix. The photophysical parameters determined are summarized in Table 1.

To elucidate the photophysics of G and G@Cap at the single-molecule level, fluorescence intensity time traces were simultaneously recorded for individual molecules of G and G@Cap in Zeonex. The typical time trace of G@Cap is shown in Fig. 2a, along with the corresponding intensity histogram (Fig. 2b) and a 0.6 s zoom of the intensity trace (Fig. 2c). The fluorescence intensity trace exhibits frequent and discrete jumps between the stable (~34 counts/0.5 ms, referred to as the "on" level) and background (~3 counts/0.5 ms, the "off" level) intensity levels before being irreversibly photobleached at 77 s. Similar on/off blinking and one-step photobleaching were also observed for the intensity traces of G (Fig. S1 in the ESI†). The fluorescence blinking of BPEA embedded in the Zeonex film has previously been assigned to triplet blinking that originates from the intersystem crossing (ISC) toward and away from the triplet state (T_1).[23] Therefore, the fluorescence blinking observed for G and G@Cap is tentatively attributed to triplet blinking.

An analysis of triplet blinking based on the three-state model of S_0, S_1, and T_1 provides the triplet lifetime (τ_T) and ISC quantum yield (Φ_{ISC}) of single molecules.[24–26] The τ_T value can be determined directly from the average off-time (τ_{off}) obtained by the histogram

Table 1 Averaged values and ranges of photophysical parameters for G, G@Cap, and R6G single-molecules embedded in a Zeonex film determined using SMFS with excitation at 488 nm.

	$\langle\lambda_{max}\rangle$ / nm	$\langle\tau_T\rangle$ / ms		Φ_{ISC}	$\langle N_{tot}\rangle$	Φ_0
		HM	ACF			
G	532 (12.5) [a]	1.12 (0.62)	1.29 (0.69)	10^{-5}~10^{-1}	9.8×10^{6}	1.9×10^{-7}
G@Cap	545 (9.9)	1.05 (0.35)	1.33 (0.32)	10^{-4}~10^{-3}	8.1×10^{7}	2.3×10^{-8}
R6G [b]	543 (15.5)	–	–	–	$\leq3.4\times10^{6}$	$\geq7.9\times10^{-7}$

[a] Values in parentheses indicate FWHMs of Gaussian fits of the histograms.
[b] Values are determined from Figs.S5 and S6 in the ESI†.

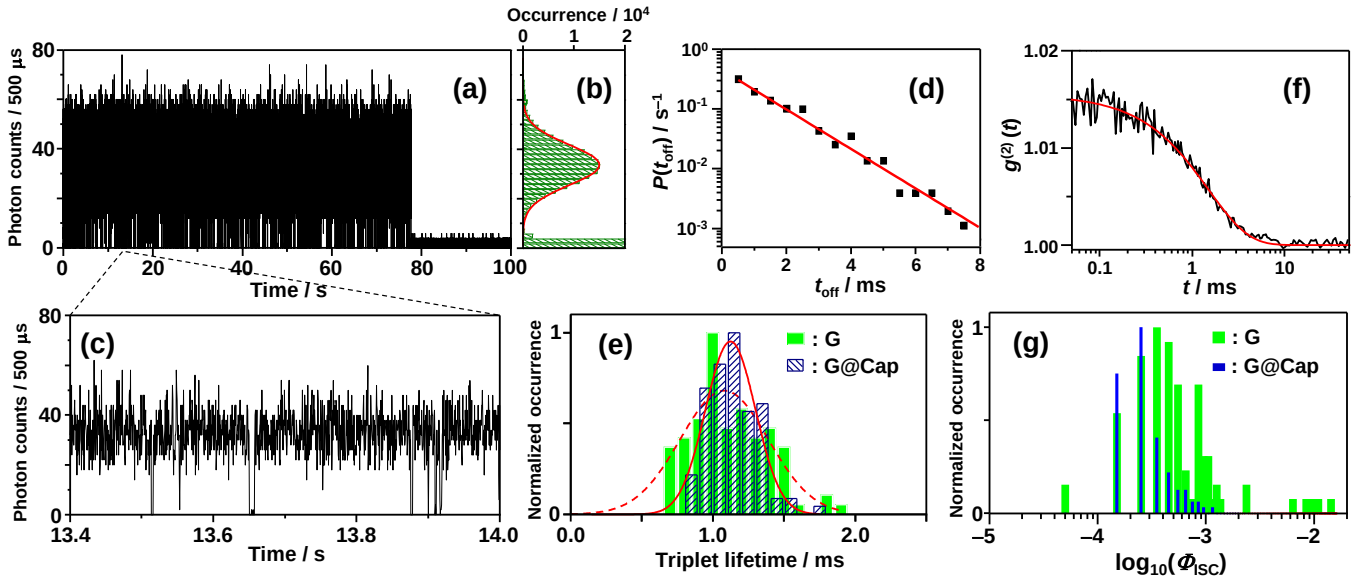

Fig. 2 (a) A fluorescence intensity trace for single G@Cap obtained with an average excitation intensity of 200 W/cm^2 and (b) the corresponding intensity histogram. (c) Fluorescence intensity trace of (a) from 13.4 to 14.0 s magnified to explicitly show on/off blinking. (d) Probability density distributions of off-time duration. Straight line is a single exponential fit. (e) Histograms of triplet lifetimes obtained from 92 G and 96 G@Cap molecules. Dotted and solid lines are Gaussian fits of each distribution. (f) Fluorescence intensity autocorrelation curve with corresponding single exponential fit. (g) Histograms of ISC yields obtained from 84 G and 90 G@Cap molecules.

method (HM) or autocorrelation function (ACF) analysis,[24–28] whereas the Φ_{ISC} value is calculated using the average on-time (τ_{on}) or on-count ($\langle N_{on}\rangle$). However, the τ_{on} and $\langle N_{on}\rangle$ values determined by the histogram method depend strongly on the selected bin time,[23] so the τ_{on} values obtained from the ACF analysis were employed to estimate Φ_{ISC} through the relation of $1/\tau_{on} = k_{ex}\Phi_{ISC}$.[24–27] In the ACF analysis, T3R mode of data collection enables us to conduct bin-time-free data analysis based on single-photon events. As evident from Fig. 2b, the intensity histogram of the "on" level displays a symmetric distribution and is satisfactorily fitted with a Gaussian function, which implies that a bin time of 500 μs is sufficient to resolve the observed blinking kinetics.[28] The unbiased threshold level (I_{th}) is determined using the equation $(I_{th} - I_{off})/I_{off}^{1/2} = (I_{on} - I_{th})/I_{on}^{1/2}$, where I_{on} and I_{off} are the average intensity levels of the "on" and "off" states, respectively.[28,29] The intensity at a given time above and below I_{th} is assigned to the "on" and "off" states, respectively. Fig. 2d shows the probability density distribution for the off-time durations (t_{off}) obtained from the intensity time trace (Fig. 2a). The distribution shows a linear dependence on t_{off} in a log-lin plot and is fitted with a single exponential function, yielding the average t_{off} (*i.e.*, τ_T = 1.32 ms). We note that the probability density distributions for the on-time durations and on-counts also exhibit single exponential distributions (Fig. S2). Because the ISC process toward (or away from) the triplet state in a single-molecule is generally characterized by monoexponential kinetics,[24–28] the results indicate that the observed blinking is caused by the ISC process. The charge transfer between G (or G@Cap) and Zeonex is unlikely, because 1) the cyclo-olefin polymer presumably possesses a very large HOMO-LUMO band gap and 2) fluorescence blinking due to charge transfer between single-molecules and a polymer matrix has been shown to result in power-law kinetics.[28,31]

The histograms of the triplet lifetimes obtained for G and G@Cap are depicted in Fig.2e. The average values obtained by fitting each histogram are comparable (*i.e.*, 1.12 ms for G and 1.05 ms for G@Cap). However, the distribution width of G@Cap is approximately one-half that of G, suggesting that the guest molecule experiences a homogeneous environment inside the capsule. Note that the ACF analysis yields triplet lifetime histograms similar to those obtained by the HM (Table 1 and Fig. S3). Fig. 2f shows the second-order correlation function $g^{(2)}(t)$ for the data in Fig. 2a. According to the three-state model, $g^{(2)}(t)$ is given by $g^{(2)}(t) = 1 + C\cdot e^{-(1/\tau off + 1/\tau on)t}$, where C is a molecular constant.[24–26] If $I_{on} >> I_{off}$, the molecular constant is represented by $C = \tau_{off}/\tau_{on}$. Using these expressions, for example, we can derive a τ_{off} ($=\tau_T$) of 1.53 ms and a τ_{on} of 98.8 ms from $g^{(2)}(t)$ in Fig. 2f. This τ_{off} value agrees well with that obtained by the histogram method (1.32 ms). The histograms of the ISC yields thus obtained from G and G@Cap are shown in Fig. 2g. A large part of Φ_{ISC} data obtained for G and G@Cap single-molecules is almost same range (*i.e.*, 10^{-4}~10^{-3}), but the distribution width of Φ_{ISC} is significantly decreased by guest encapsulation; 10^{-5}–10^{-1} for G and 10^{-4}–10^{-3} for G@Cap. The reported fluorescence quantum yields (*i.e.*, 0.97 for G and 0.94 for G@Cap in toluene[20]) suggest that the quantum yield of non-radiative pathways is 0.03 for G and 0.06 for G@Cap, which are several orders of magnitude larger than the Φ_{ISC} values obtained herein. Therefore, it is presumed that the internal conversion from S_1 to S_0 is the main non-radiative pathway in G and G@Cap. In addition to the comparable triplet-state photophysical parameters (*e.g.*, τ_T and Φ_{ISC})

between G and G@Cap, their fluorescence lifetimes are also almost same; 2.7 ns for G and 2.9 ns for G@Cap in deaerated toluene. These facts indicate that the radiative and non-radiative pathways of the guest are mostly not affected by encapsulation. Thus, the electronic coupling between G and Cap is considered to be very weak. Indeed, the red shifts in absorption and fluorescence spectra upon encapsulation have been attributed to the structural planarization of G in the Cap, *i.e.*, geometric factor.[20] As for τ_T, the small variety of the Φ_{ISC} values for G@Cap thereby originates from a reduced structural heterogeneity (*i.e.*, conformational restriction) of G upon encapsulation and a homogeneous environment in the capsule's interior.

Enhancement of photostability of G upon encapsulation has been qualitatively reported in ref. 20. Herein, we provide its quantitative evaluation at the single-molecule level. Our single-molecule measurements at a low irradiance (~100 W/cm^2) reveal that the averaged survival lifetime $\langle t_{sur} \rangle$ of G@Cap is 210 s, which is about 11 times longer than that of free G (Figs. S4 in the ESI†). However, this result only shows *qualitative* photostability, because the number of excitation-deexcitation cycles is not taken into account in the survival time. To obtain quantitative insights into the effect of encapsulation on the photostability of a single G molecule, the photobleaching quantum yield Φ_b, defined as $\Phi_b = \xi\Phi_f/N$, is thus evaluated.[30–32] In this expression, ξ represents the overall detection efficiency of the current microscope setup (~4%), Φ_f is the fluorescence quantum yield, and N is the total number of detected photons each single molecule emits before being photobleached. The Φ_f values for G and G@Cap in toluene are 0.97 and 0.94, respectively;[20] these values are used to calculate Φ_b. The histograms of Φ_b for G and G@Cap obtained at an excitation power of 200 W/cm^2 are shown in Figs. 3a and 3b, respectively. Assuming a Poisson distribution of photobleaching events over time, the probability density function of a molecule having a certain Φ_b is given by $P(\Phi_b) = C\cdot\exp(-\Phi_0/\Phi_b)/\Phi_b^2$, where Φ_0 is a quantity for the photostability of a single molecule, and C is a normalization constant.[32] The histograms are fitted with this function (Fig. 3). From this, Φ_0 values of 1.9×10^{-7} and 2.3×10^{-8} are obtained for G and G@Cap, respectively, revealing a dramatic increase (8-fold) in the photostability upon encapsulation. It is further noted that Φ_0 value of R6G, which is a widely used fluorescent dye in single-molecule studies,[9,14,33,34] has been determined to be 7.9×10^{-7} under the same experimental conditions (Figs. S5 and S6). Therefore, G@Cap is at least 34-fold more stable than R6G.

The increase in photostability upon encapsulation indicates that the sterical protection of the anthracene framework by the cavitand capsule effectively prohibits photochemical oxidation reactions of G with, most likely, singlet oxygen $O_2(^1\Delta_g)$. The single oxygen can be produced by quenching of the long-lived triplet state of G (~1 ms), because the lowest triplet energy (153 kJ/mol, obtained at TD-B3LYP/6-31G(d)//HF/6-31G(d) level of theory) is much higher than the energy of $O_2(^1\Delta_g)$ (94 kJ/mol). Note, however, that photobleaching events are ultimately observed for all the single G@Cap molecules embedded in the Zeonex film. Since it is expected to be difficult for the G molecule tightly encapsulated in Cap to produce a 9,10-endoperoxide product having a bent molecular structure, the observed photobleaching implies that the linkers in Cap may partially (or completely) dissociate, thus allowing for the formation of 9,10-endoperoxide in the anthracene core. While the details of the mechanism of photobleaching are yet to be unraveled, the suppression of linker dissociation in Cap and/or triplet blinking of the encapsulated guest will further improve the photostability of the guest fluorophore.

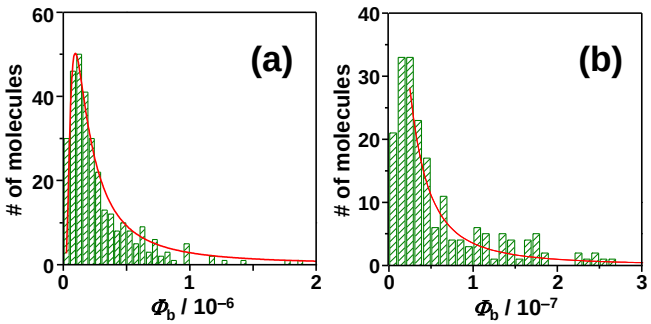

Fig.3 Histograms of photobleaching quantum yields of (a) G (312 molecules) and (b) G@Cap (200 molecules).

Conclusions

In summary, the effects of supramolecular encapsulation on the photophysics and photostability of a very bright BPEA derivative having excellent optical properties are examined by SMFS. The distribution of triplet-state kinetics discloses a relatively homogeneous environment in the capsule's interior. The analysis of single-molecule photobleaching behavior quantitatively demonstrates that the encapsulation using the self-assembled boronic ester cavitand capsule leads to a nearly 10-fold enhancement in the longevity of the guest fluorophore. Furthermore, this encapsulation complex is >30-fold more photostable than R6G in a glassy polymer environment. Hence, this encapsulation complex is expected to serve as a very photostable one-photon (and probably two-photon) fluorescent probe for potential applications in various research areas where single-molecule detection is demanded.

Acknowledgements

M.M is grateful to Mr. Takeo Saito from Shimadzu Corporation is acknowledged grateful for experimental work with AFM. This work is partly supported by Grant-in-Aids for Young Scientists (A), No. 20685001, Scientific Research on Priority Areas "Molecular Science for Supra Functional Systems", No. 20050011.

Notes and references

Department of Chemistry, Graduate School of Science, Shizuoka University, 836 Ohya, Suruga-ku, Shizuoka 422-8529, Japan.
E-mail: smmitsu@ipc.shizuoka.ac.jp; Tel: +81-54-238-4755

† Electronic Supplementary Information (ESI) available: [Additional data, including the fluorescence intensity trace of single G molecules, the probability density distributions of on-time duration and on-counts for single G@Cap, the histograms of triplet lifetimes obtained from the

autocorrelation analysis, the histograms of $\langle t_{sur} \rangle$ for G and G@Cap, the histograms of λ_{max} and Φ_b of R6G]. See DOI: 10.1039/b000000x/

1 M. Sauer, J. Hofkens, J. Enderlein, *Handbook of Fluorescence Spectroscopy and Imaging*; Wiley-VCH Verlag GmbH&Co. KGaA, Weinheim, 2011.

2 T. Weil, T. Vosch, J. Hofkens, K. Peneva, K. Müllen, The Rylene Colorant Family-Tailored Nanoemitters for Photonics Research and Applications, *Angew. Chem. Int. Ed.* 2010, **49**, 9068.

3 T. Züchner, A. V. Failla, A. J. Meixner, Light Microscopy with Doughnut Modes: A Concept to Detect Characterize, and Manipulate Individual Nanoobjects, *Angew. Chem. Int. Ed.* 2011, **50**, 5274.

4 R. Kasper, B. Harke, B. C. Forthmann, P. Tinnerfeld, S. W. Hell, M. Sauer, Single-Molecule STED Microscopy with Photostable Organic Fluorophores, *Small* 2010, **6**, 1379.

5 R. B. Altman, Q. Zheng, Z. Zhou, D. S. Terry, J. D. Warren, S. C. Blanchard, Enhanced Photostability of Cyanine Fluorophores Across the Visible Spectrum, *Nat. Methods* 2012, **9**, 428.

6 Q. Zheng, S. Jockusch, Z. Zhou, R. B. Altman, J. D. Warren, N. J. Turro, S. C. Blanchard, On the Mechanisms of Cyanine Fluorophore Photostabilization, *J. Phys. Chem. Lett.* 2012, **3**, 2200.

7 J. Vogelsang, R. Kasper, C. Steinhauer, B. Person, M. Heilemann, M. Sauer, P. Tinnefeld, A Reducing and Oxidizing System Minimizes Photobleaching and Blinking of Fluorescent Dyes, *Angew. Chem., Int. Ed.* 2008, **47**, 5465.

8 E. Lemke, Y. Gambin, V. Vandelinder, E. M. Brustad, H-W. Liu, P. G. Schultz, A. Groisman, A. A. Deniz, Microfluidic Device for Single-Molecule Experiments with Enhanced Photostability, *J. Am. Chem. Soc.* 2009, **131**, 13610.

9 L. Guo, F. Gai, Simple Method to Enhance the Photostability of the Fluorescence Reporter R6G for Prolonged Single-Molecule Studies, *J. Phys. Chem. A* 2013, **117**, 6164.

10 M. T. Stone, H. L. Anderson, A Cyclodextrin–Insulated Anthracene Rotaxane with Enhanced Fluorescence and Photostability, *Chem. Commun*. 2007, 2387.

11 J. S. Park, J. N. Wilson, K. I. Hardcastle, U. H. F. Bunz, M. Srinivasarao, Reduced Fluorescence Quenching of Cyclodextrin−Acetylene Dye Rotaxanes, *J. Am. Chem. Soc.* 2006, **128**, 7714.

12 M. J. Frampton, H. L. Anderson, Insulated Molecular Wires, *Angew. Chem., Int. Ed.* 2007, **46**, 1028.

13 J. Mohanty, W. M. Nau, Ultrastable Rhodamine with Cucurbituril, *Angew. Chem. Int. Ed*. 2005, **44**, 3750.

14 T. A. Martyn, J. L. Moore, R. L. Halterman, W. T. Yip, Cucurbit[7]uril Induces Superior Probe Performance for Single-Molecule Detection, *J. Am. Chem. Soc.* 2007, **129**, 10338.

15 E. Arunkumar, C.C. Forbes, B. C. Noll, B. D. Smith, Squaraine-Derived Rotaxanes: Sterically Protected Fluorescent Near-IR Dyes, *J. Am. Chem. Soc.* 2005, **127**, 3288.

16 M. R. Ams, D. Ajami, S. L. Craig, J-S. Yang, Jr. J. Rebek, "Too Small, Too Big, and Just Right" – Optical Sensing of Molecular Conformations in Self-Assembled Capsules, *J. Am. Chem. Soc.* 2009, **131**, 13190.

17 N. Nishimura, K. Kobayashi, Self-Assembly of a Cavitand-Based Capsule by Dynamic Boronic Ester Formation, *Angew. Chem. Int. Ed.* 2008, **47**, 6255.

18 N. Nishimura, K. Yoza, K. Kobayashi, Guest-Encapsulation Properties of a Self-Assembled Capsule by Dynamic Boronic Ester Bonds, *J. Am. Chem. Soc.* 2010, **132**, 777.

19 N. Nishimura, K. Kobayashi, Self-Assembled Boronic Ester Cavitand Capsule as a Photosensitizer and a Guard Nanocontainer against Photochemical Reactions of 2,6-Diacetoxyanthracene, *J. Org. Chem.* 2010, **75**, 6079.

20 Y. Hirumi, K. Tamaki, T. Namikawa, K. Kamada, M. Mitsui, K. Suzuki, K. Kobayashi, Encapsulation with Protrusion of Cruciform 9,10-Bis(arylethynyl)anthracene Derivatives in a Self-Assembled Boronic Ester Cavitand Capsule: Photochemical and Photophysical Properties, *Chem. Asian J.* accepted for publication

21 M. Levitus, M. A. Garcia-Garibay, Polarized Electronic Spectroscopy and Photophysical Properties 9,10-Bis(phenylethynyl)anthracene, *J. Phys. Chem. A* 2000, **104**, 8632.

22 A. Beeby, K. S. Findlay, A. E. Goeta, L. Porrès, L. S. R. Rutter, A. L. Thompson, Engineering a Twist in 9,10-Diethynylanthracenes by Steric Interactions, *Photochem. Photobiol. Sci.* 2007, **6**, 982.

23 M. Mitsui, Y. Kawano, R. Takahashi, H. Fukui, Photophysics and Photostability of 9,10-Bis(phenylethynyl)anthracene Revealed by Single-Molecule Spectroscopy, *RSC Adv*. 2012, **2**, 9921.

24 T. Ha, Th. Enderle, D. S. Chemla, P. R. Selvin, S. Weiss, Quantum Jumps of Single Molecules at Room Temperature, *Chem. Phys. Lett.* 1997, **271**, 1.

25 W. -T. Yip, D. Hu, J. Yu, D. A. V. Bout, P. F. Barbara, Classifying the Photophysical Dynamics of Single- and Multiple-Chromophoric Molecules by Single Molecule Spectroscopy, *J. Phys. Chem. A* 1998, **102**, 7564.

26 K. D. Weston, P. J. Carson, J. A. DeAro, S. K. Buratto, Single-Molecule Detection Fluorescence of Surface-Bound Species in Vacuum, *Chem. Phys. Lett.* 1999, **308**, 58.

27 D. S. English, E. J. Harbron, P. F. Barbara, Probing Photoinduced Intersystem Crossing by Two-Color, Double Resonance Single Molecule Spectroscopy, *J. Phys. Chem. A* 2000, **104**, 9057.

28 M. Hasse, C. G. Hübner, E. Reuther, E. A. Herrmann, K. Müllen, T. Baschè, Exponential and Power-Law Kinetics in Single-Molecule Fluorescence Intermittency, *J. Phys. Chem. B* 2004, **108**, 10445.

29 M. Lippitz, F. Kulzer, M. Orrit, Stastistical Evaluation of Single Nano-Object Fluorescence, *ChemPhysChem* 2005, **6**, 770.

30 W. P. Ambrose, P. M. Goodwin, J. C. Martin, Keller, R. A. Single Molecule Detection and Photochemistry on a Surface Using Near-Field Optical Excitation, *Phys. Rev. Lett.* 1994, **72**, 160.

31 M. Hasse, C. G. Hübner, F. Nolde, K. Müllen, T. Baschè, Photoblinking and Photobleaching of Rylene Diimide Dyes, *Phys. Chem. Chem. Phys.* 2011, **13**, 1776.

32 M. Nothaft, S. Höhla, F. Jelezko, J. Pflaum, J. Wrachtrup, The Role of Oxygen-Induced Processes on the Emission Characteristics of Single Molecule Emitters, *Phys. Staus Solidi B* 2012, **249**, 661.

33 D. K. Das, T. Mondal, A.1K. Mandal, K. Bhattacharyya, Binding of Organic Dyes with Human Serum Albumin: A Single-Molecule Study, *Chem. Asian J.* 2011, **6**, 3097.

34 N. Z. Wong, A. F. Ogata, K. L. Wustholz, Dispersive Electron-Transfer Kinetics from Single Molecules on TiO_2 Nanoparticle Films, *J. Phys. Chem. C* 2013, **117**, 21075.

Graphical Abstract

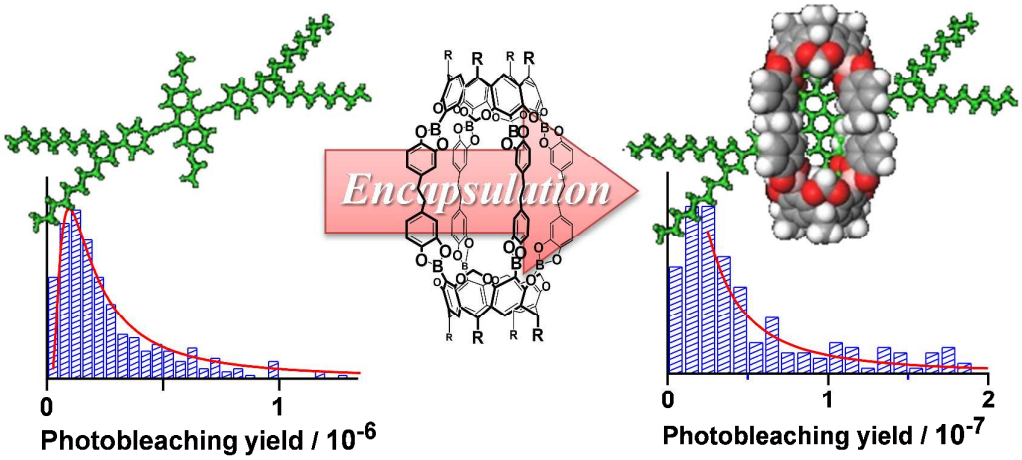

Short statement of novelty for publication

Single-molecule study of an anthracene-based dye and its supramolecular encapsulation complex revealed a 10-fold increase in the photostability of the guest due to encapsulation. This complex is >30-fold more photostable than rhodamine 6G.